Electronic Supplementary Information

Rationally designed hierarchical N-doped carbon@$NiCo_2O_4$ double-shelled nanoboxes for enhanced visible light CO_2 reduction

*Sibo Wang, Bu Yuan Guan and Xiong Wen (David) Lou**

School of Chemical and Biomedical Engineering, Nanyang Technological University,

62 Nanyang Drive, Singapore, 637459, Singapore

E-mail: xwlou@ntu.edu.sg; davidlou88@gmail.com

Experimental details

Synthesis of Fe_2O_3 nanocubes. The Fe_2O_3 nanocubes were synthesized according to a modified hydrothermal method.[1] Typically, 25 mL of 2.0 M $FeCl_3 \cdot 6H_2O$ solution was stirred in an oil bath at 75 °C for 5 min. Then, 25 mL of 5.4 M NaOH solution was added by a syringe with a rate of 10 mL min^{-1}. After stirring at the same temperature for 10 min, the obtained $Fe(OH)_3$ gel was maintained in a preheated oven at 100 °C for 4 days. The red product was collected and washed three times with deionized (DI) water and ethanol, and dried at 70 °C for 12 h.

Synthesis of Fe_2O_3@PDA core-shelled nanocubes. 320 mg of the Fe_2O_3 nanocube template was homogeneously dispersed in Tris-buffer solution (400 mL, 10 mM) by sonication for 30 min, followed by the addition of 160 mg of dopamine hydrochloride and stirred for 3 h. The resultant Fe_2O_3@PDA product was collected by centrifugation, washed with DI water and ethanol three times, and dried at 70 °C for 12 h.

Synthesis of N-doped carbon (NC) nanoboxes. 160 mg of the Fe_2O_3@PDA core-shelled nanocubes were annealed in N_2 at 500 °C for 3 h with a heating rate of 5 °C min^{-1}. Then, the annealed product was dispersed in 100 mL of 4 M HCl solution and stirred at 70 °C for 1 h to completely remove the template. The obtained NC nanoboxes were collected by centrifugation, washed with ethanol three times, and then further annealed in N_2 at 700 °C for 2 h with a heating rate of 5 °C min^{-1}.

Synthesis of hierarchical NC@$NiCo_2O_4$ double-shelled nanoboxes. 10 mg of NC nanoboxes was first dispersed in 10 mL of ethanol solution containing 200 mg of polyvinylpyrrolidone (PVP, M_w = 40000) and stirred for 12 h. The PVP-functionalized NC nanoboxes were collected by centrifugation, and washed with ethanol. Then, the resultant PVP-modified NC nanoboxes were dispersed in 10 mL of ethanol and 40 mL of H_2O by sonication for 30 min, followed by the addition of 0.1 mmol of $Ni(NO_3)_2 \cdot 6H_2O$ and 0.2 mmol of $Co(NO_3)_2 \cdot 6H_2O$. After stirring for 5 min, 0.5 mmol of hexamethylenetetramine and 0.05 mmol of trisodium citrate was added to the mixture and stirred for 10 min. The resultant mixture was refluxed in an oil bath at 90 °C for 6 h with rigorous stirring. After cooling down to room temperature, the NC@Ni-Co LDH precursor was harvested by centrifugation, washed with ethanol three times, and dried at 70 °C for 12 h. Finally, the precursor was further annealed in air at 300 °C with a heating rate of 5 °C min^{-1} to harvest the hierarchical NC@$NiCo_2O_4$ double-shelled nanoboxes.

Materials characterization. Field-emission scanning electron microscope (FESEM; JEOL-6700) and transmission electron microscope (TEM; JEOL, JEM-2010) were used to examine the morphology and structure of the samples. The crystal phases of the samples were analyzed by X-ray diffraction (XRD) on a Bruker D2 Phaser X-Ray Diffractometer with Ni filtered Cu $K\alpha$ radiation (λ = 1.5406 Å) at a voltage of 30 kV and a current of 10 mA. The compositions of the samples were analyzed by energy-dispersive X-ray spectroscope (EDX) attached to the FESEM instrument. Elemental mapping images were recorded using EDX spectroscope attached to TEM (JEOL, JEM-2100F). X-ray photoelectron spectra (XPS) were collected on a PHI Quantum 2000 XPS system with the C 1s peak (284.6 eV) as a reference. N_2 adsorption measurements were taken on a Micromeritics ASAP 2020 system at liquid N_2 temperature. Specific surface area was determined by the Brunauer-Emmett-Teller (BET) method. N_2 and CO_2 adsorption isotherms were collected on an ASAP2020M apparatus. The samples were degassed in vacuum at 120 °C for 12 h and then measured at 77 K and 0 °C, respectively. UV-vis diffuse reflectance spectra (DRS) were obtained using a Varian Cary 500 UV-vis-NIR spectrometer equipped with an integrating sphere and $BaSO_4$ was used as reference. Photoluminescence (PL) spectra were performed on Edinburgh Analytical Instruments FL/FSTCSPC920 coupled with a time-correlated single-photo-counting system at room temperature. An Agilent 7820A gas chromatograph (GC) equipped with a thermal conductivity detector (TCD)

and a packed column (TDX-01) was utilized to analyze and quantify the gases produced from the CO_2 photoreduction system with Ar as the carrier gas. An HP 5973 gas chromatography-mass spectrometer (GC-MS) was employed to analyze the gaseous products generated from the $^{13}CO_2$ (97% enriched) isotopic experiment and to determine whether other potential products were generated in the liquid phase. The used column in GC-MS analysis for the products of the isotopic experiments is HP-MOLESIEVE (30 m × 0.32 mm, Agilent Technologies, Serial number: USD 130113H). The temperature of the inlet and oven is 200 °C and 45 °C, respectively. The carrier gas is helium (He) with a flow of 0.6 mL min^{-1}.

Photocatalytic CO_2 reduction. In the typical photocatalytic CO_2 reduction reaction, NC@$NiCo_2O_4$ (1 mg), $[Ru(bpy)_3]Cl_2·6H_2O$ (10 μmol, abbreviated as **Ru**, bpy = 2'2-bipyridine), solvent (5 mL, H_2O/acetonitrile, V/V = 2:3), and triethanolamine (TEOA, 1 mL) were added in a gas-closed glass reactor (80 mL in capacity). Then, high purity CO_2 was introduced to the reactor with a partial pressure of 1 atm. A 300W Xe lamp with a 420 nm cutoff filter was used as the light source. The temperature of the reaction system was kept at 30 °C by cooling water. During the photocatalytic process, the reaction system was vigorously stirred with a magnetic stirrer. After reaction for a certain time, the generated products were sampled and quantified by an Agilent 7820A gas chromatograph.

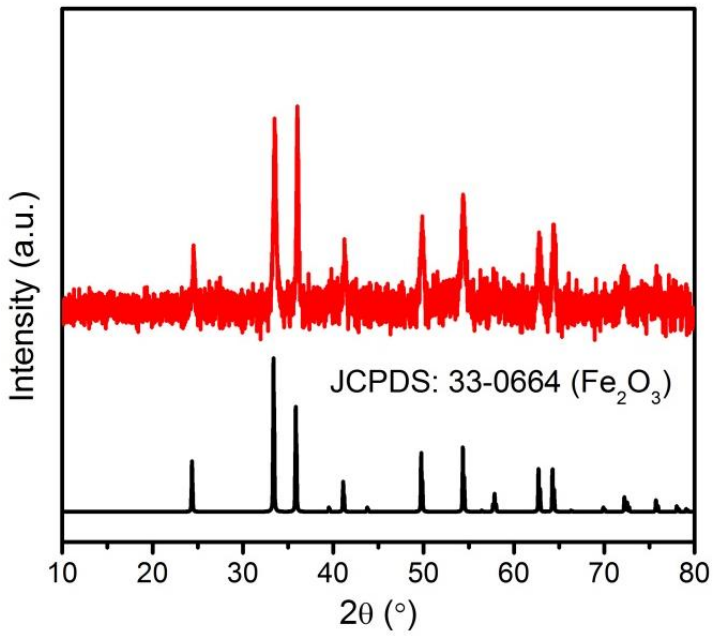

Fig. S1 XRD pattern of Fe_2O_3 nanocubes.

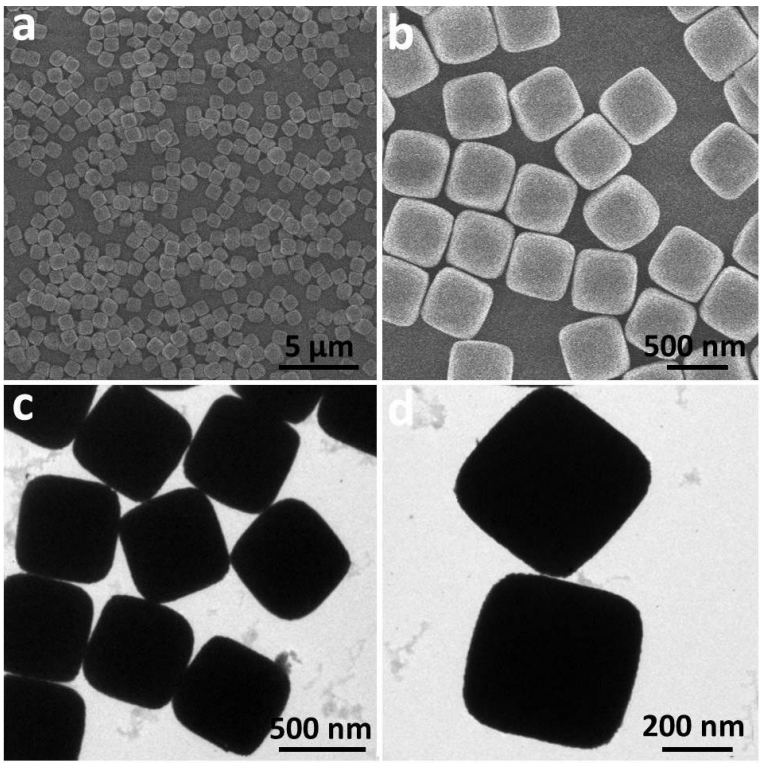

Fig. S2 (a,b) FESEM and (c,d) TEM images of Fe_2O_3 nanocubes.

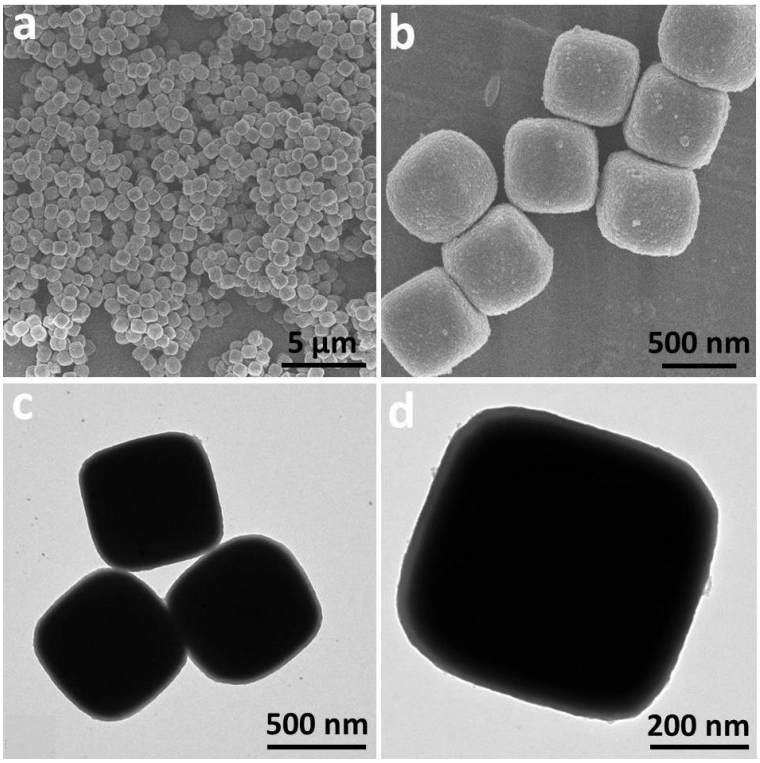

Fig. S3 (a,b) FESEM and (c,d) TEM images of Fe_2O_3@PDA core-shelled nanocubes.

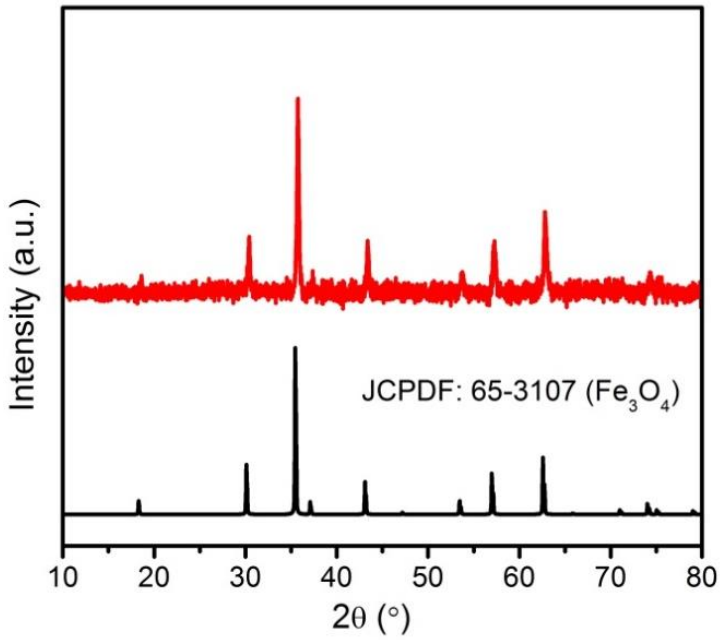

Fig. S4 XRD pattern of Fe_3O_4@NC core-shelled nanocubes.

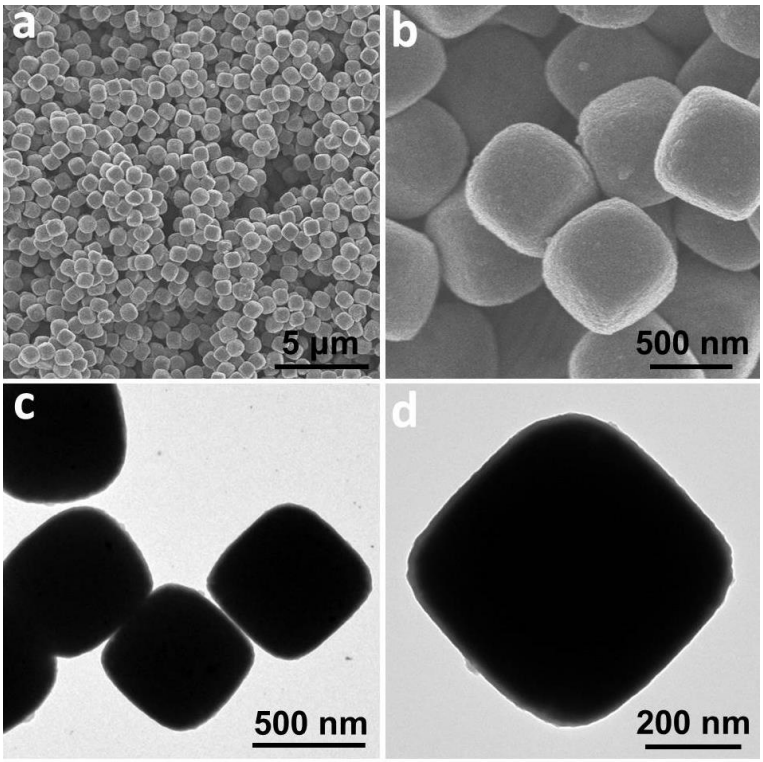

Fig. S5 FESEM and (c,d) TEM images of Fe_3O_4@NC core-shelled nanocubes.

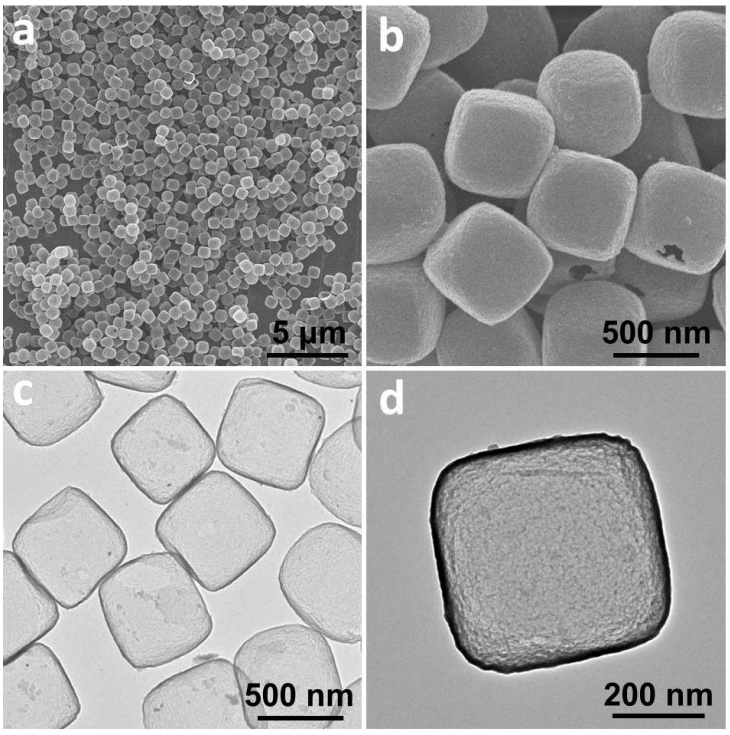

Fig. S6 (a,b) FESEM and (c,d) TEM images of NC nanoboxes.

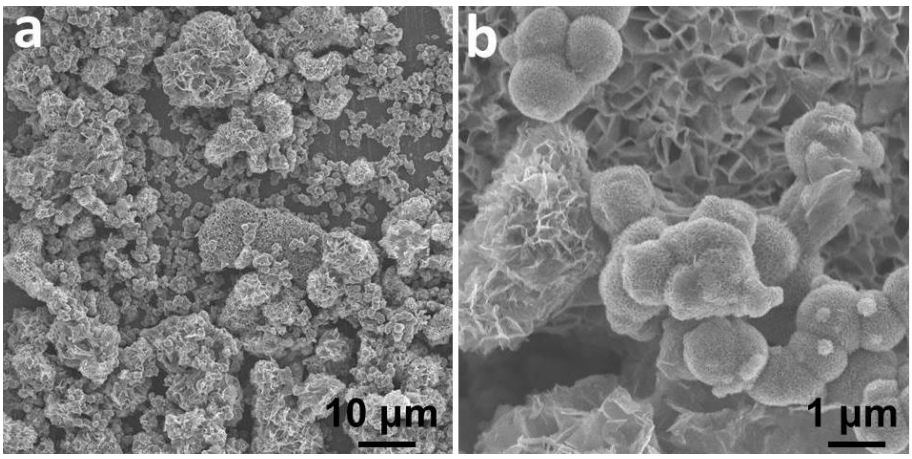

Fig. S7 FESEM images of the bulk $NiCo_2O_4$ particles synthesized in absence of NC nanoboxes.

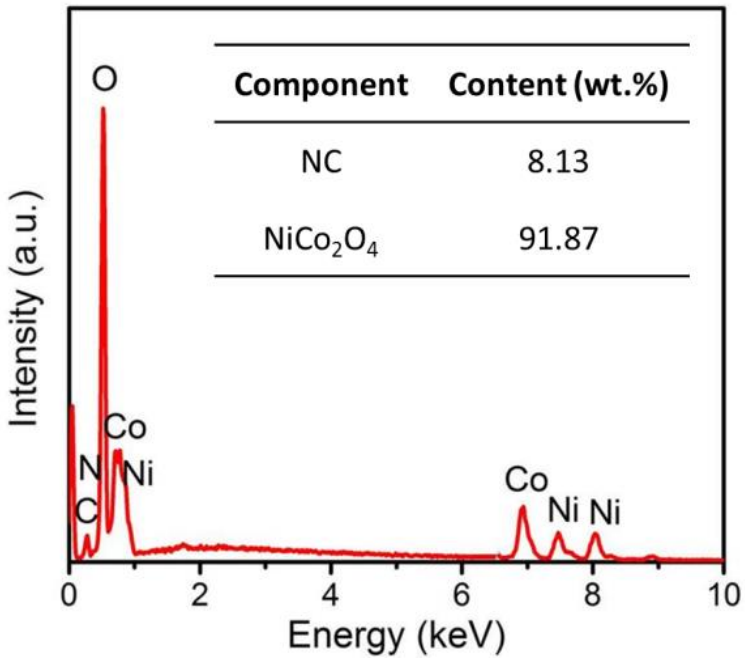

Fig. S8 EDX spectrum of hierarchical NC@$NiCo_2O_4$ double-shelled nanoboxes.

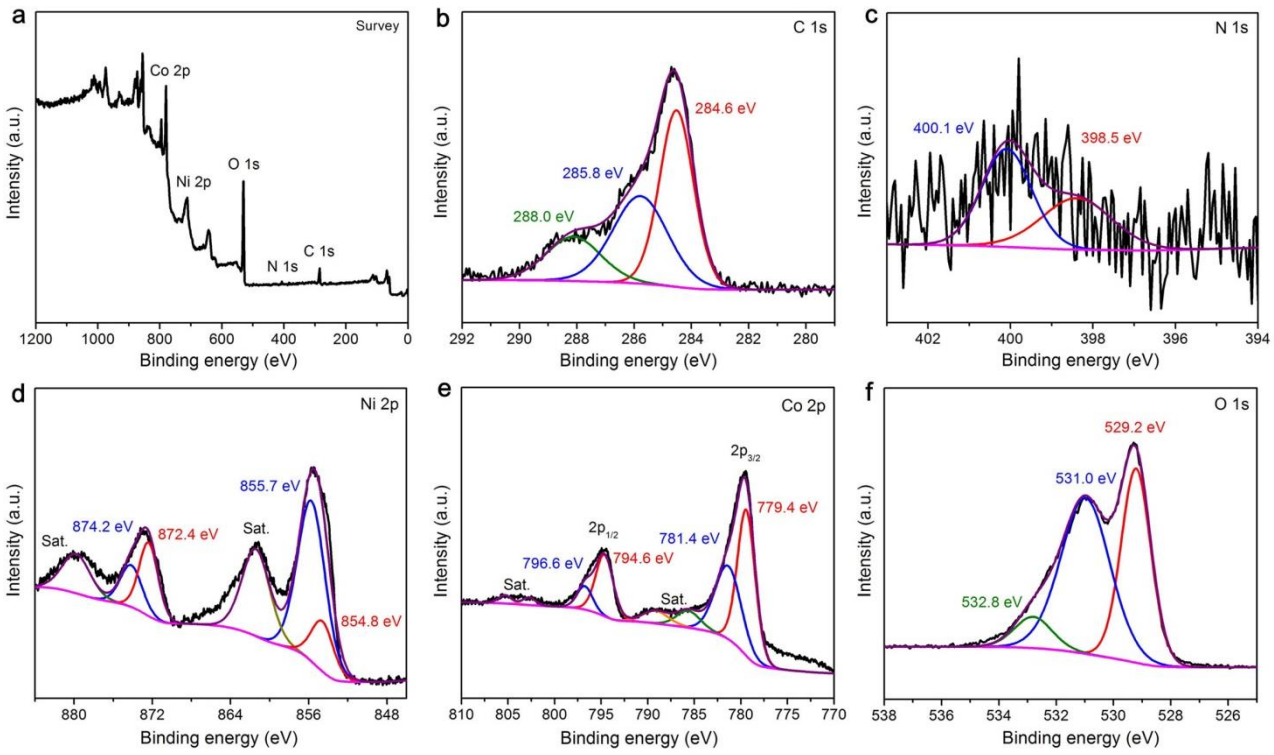

Fig. S9 XPS spectra of hierarchical NC@$NiCo_2O_4$ double-shelled nanoboxes: (a) survey spectrum and high resolution spectra of (b) C 1s, (c) N 1s, (d) Ni 2p, (e) Co 2p, and (f) O 1s.

The survey spectrum gives the signals of C, N, Ni, Co and O elements (Fig. S9a), consistent with the results of EDX tests (Fig. S8). The XPS spectrum of C 1s can be divided into three peaks (Fig. S9b). The main peak at 284.6 eV corresponds to the graphite-like sp^2 C, and the small peaks at 285.8 and 288.0 eV are attributed to the N-sp^2 C and N-sp^3 C bonds, respectively.[2] The N 1s XPS spectrum can be deconvoluted into two peaks at binding energies of 398.5 and 400.1 eV (Fig. S9c), corresponding to C-N and C=N bonds, respectively.[3,4] The high-resolution Ni 2p spectrum is well fitted considering two spin-orbit double characteristic of Ni^{2+} and Ni^{3+} with binding energy at 854.8 eV, 872.4 eV and 855.7 eV, 874.2 eV (Fig. S9d), respectively.[5] The peaks at around 861.3 and 879.8 eV are indexed to the two shake-up satellites of nickel. In the Co 2p spectrum (Fig. S9e), two kinds of Co species are detected. The binding energy at 779.4 eV and 794.6eV are ascribed to Co^{3+}, and the binding energy at 781.4 eV and 796.6 eV are assigned to Co^{2+}.[5,6] In the XPS spectrum of O 1s (Fig. S9f), the three peaks centered at 529.2, 531.0 and 532.8 eV are correspondingly attributed to the lattice oxygen, the oxygen of hydroxide ions, and the oxygen of physically adsorbed water molecules.[5,7]

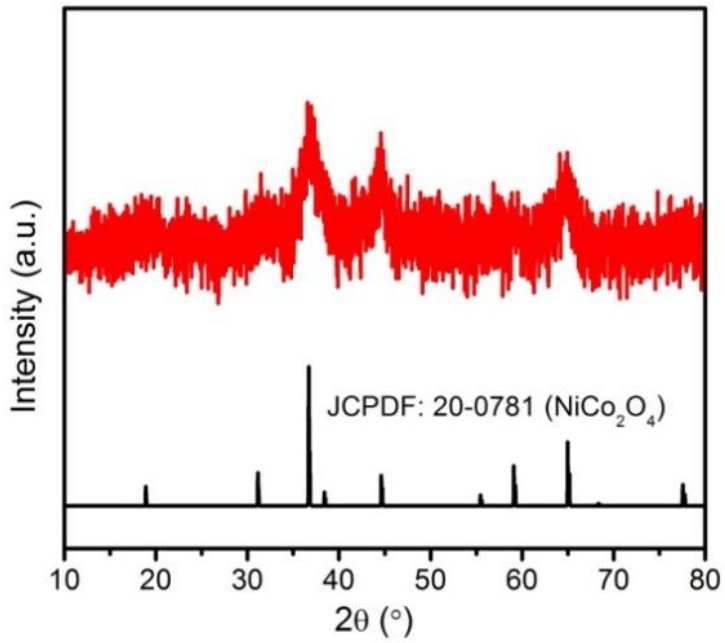

Fig. S10 XRD pattern of hierarchical NC@$NiCo_2O_4$ double-shelled nanoboxes.

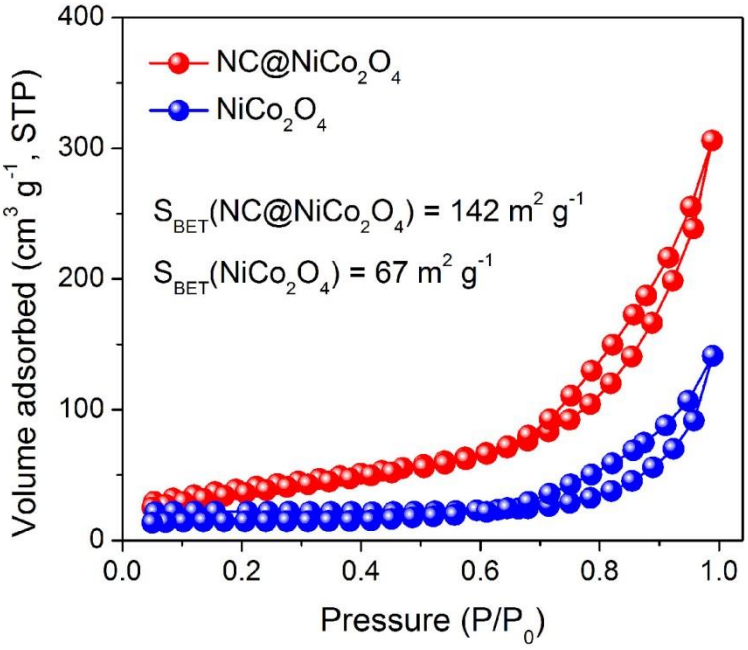

Fig. S11 N_2 sorption isotherms and BET surface areas of NC@$NiCo_2O_4$ nanoboxes and bulk $NiCo_2O_4$ particles.

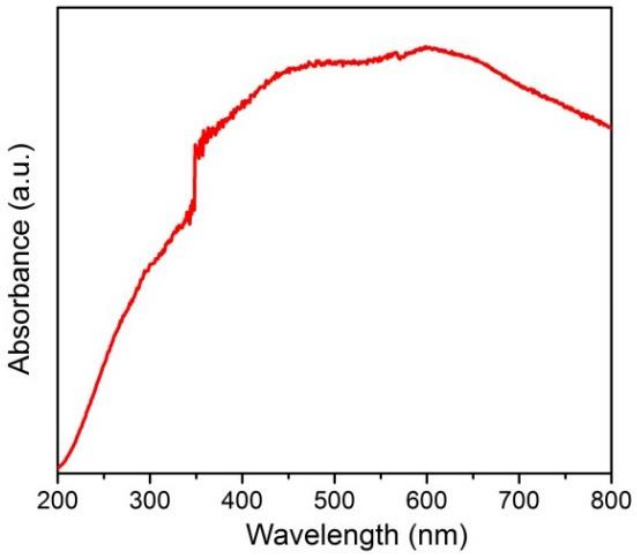

Fig. S12 UV-Vis diffuse reflectance spectrum (DRS) of hierarchical NC@$NiCo_2O_4$ double-shelled nanoboxes.

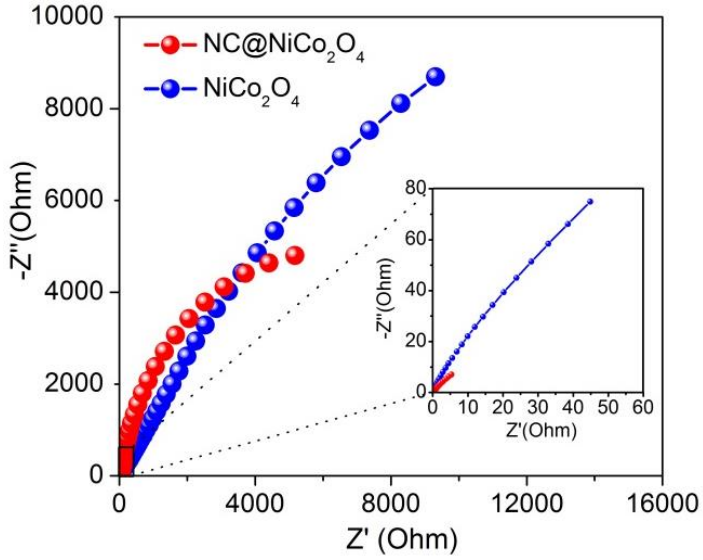

Fig. S13 Nyquist plots of hierarchical NC@$NiCo_2O_4$ double-shelled nanoboxes and bulk $NiCo_2O_4$ particles.

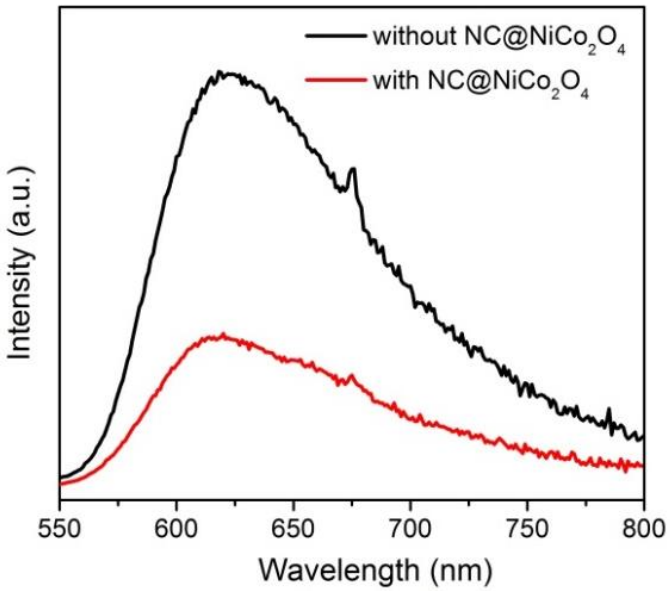

Fig. S14 PL spectra of the photocatalytic CO_2 reduction systems with and without hierarchical NC@$NiCo_2O_4$ double-shelled nanoboxes as the catalyst under 500 nm laser irradiation at room temperature.

Table S1. Comparison of photocatalytic CO_2 conversion performance.

Catalyst (used amount)	Cocatalyst sacrificial agent	Major product evolution rate (μmol h^{-1}) [a]	Reference
NC@$NiCo_2O_4$ (1 mg)	$Ru(bpy)_3^{2+}$ TEOA	**CO: 26.2**	**This work**
Co_3O_4 (10 mg)	$Ru(bpy)_3^{2+}$ TEOA	CO: 20.03	8
Ni(TPA/TEG) (1 mg)	$Ru(bpy)_3^{2+}$ TEOA	CO: 26.6	9
MAF-X27/*I*-OH (1.77 mg)	$Ru(bpy)_3^{2+}$ TEOA	CO: 14	10
$CoSn(OH)_6$ (1 mg)	$Ru(bpy)_3^{2+}$ TEOA	CO: 18.7	11
$[Co_2(OH)\mathbf{L^1}](ClO_4)_3$ (0.025 μM)	$[Ru(phen)_3](PF_6)_2$ TEOA	CO: 2.11	12
BCN (50 mg)	$Co(bpy)_3^{2+}$ TEOA	CO: 4.7	13
HR-CN (30 mg)	$Co(bpy)_3^{2+}$ TEOA	CO: 8.9	14
Zr-bpdc/**RuCO** (2.9 mg)	$Ru(bpy)_3^{2+}$ TEOA	CO: 6.75 HCCOH: 23.175	15
N-Ta_2O_5 (50 mg)	$[Ru(dcbpy)_2(CO)_2]^{2+}$ TEOA	HCOOH: 3.5	16
RuRu'/mpg-C_3N_4 (4 mg)	Ag EDTA·2Na	$COOH^-$: 8.46	17
RuRu'/NS-C_3N_4 (4 mg)	Ag EDTA·2Na	$COOH^-$: 0.23	18
MOF-525-Co (2 mg)	/ TEOA	CO: 0.403 CH_4: 0.07	19
UiO-66/CNNS (1000 mg)	/ TEOA	CO: 9.79	20
NH_2-MIL-125(Ti) (50 mg)	/ TEOA	$COOH^-$: 2	21
PCN-222 (50 mg)	/ TEOA	$COOH^-$: 6.25	22

[a] Product evolution rate is calculated based on the added amount of catalyst in CO_2 reduction system.

Supplementary References

1. X. Y. Yu, H. Hu, Y. Wang, H. Chen and X. W. Lou, *Angew. Chem. Int. Ed.*, 2015, **54**, 7395.
2. F.Yang, Z. Zhang , K. Du, X. Zhao, W. Chen, Y. Lai and J. Li, *Carbon*, 2015, **91**, 88.
3. L. Zhao, Y. S. Hu, H. Li, Z. Wang and L. Chen, *Adv. Mater.*, 2011, **23**, 1385.
4. Y. Ma, C. Zhang, G. Ji and J. Y. Lee, *J. Mater. Chem.*, 2012, **22**, 7845.
5. Z. Wang, M. Jiang, J. Qin, H. Zhou and Z. Ding, *Phys. Chem. Chem. Phys.*, 2015, **17**, 16040.
6. L. Qian, L. Gu, L. Yang, H. Y. Yuan and D. Xiao, *Nanoscale*, 2013, **5**, 7388.
7. R. J. Zou, K. B. Xu, T. Wang, G. J. He, Q. Liu, X. J. Liu, Z. Y. Zhang and J. Q. Hu, *J. Mater. Chem. A*, 2013, **1**, 8560.
8. C. Gao, Q. Meng, K. Zhao, H. Yin, D. Wang, J. Guo, S. Zhao, L. Chang, M. He, Q. Li, H. Zhao, X. Huang, Y. Guo and Z. Tang, *Adv. Mater.,* 2016, **28**, 6485.
9. K. Niu, Y. Xu, H. Wang, R. Ye, H. L. Xin, F. Lin, C. Tian, Y. Lum, K. C. Bustillo, M. M. Doeff, M. T. M. Koper, J. Ager, R. Xu and H. Zheng, *Sci. Adv.*, 2017, **3**, e1700921.
10. Y. Wang, N. Y. Huang, J. Q. Shen, P. Q. Liao, X. M. Chen and J. P.Zhang, *J. Am. Chem. Soc.*, 2018, DOI: 10.1021/jacs.7b10107.
11. X. Lin, Y.Gao, M. Jiang, Y. Zhang, Y. Hou, W. Dai, S. Wang and Z. Ding, *Appl. Catal. B Environ.*, 2018, **224**, 1009.
12. T. Ouyang, H. H. Huang, J. W. Wang, D. C. Zhong and T. B. Lu, *Angew. Chem. Int. Ed.*, 2017, **56**, 738.
13. C. Huang, C. Chen, M. Zhang, L. Lin, X. Ye, S. Lin, M. Antonietti and X. Wang, *Nat. Commun.*, 2015, **6**, 7698.
14. Y. Zheng, L. Lin, X. Ye, F. Guo and X. Wang, *Angew. Chem. Int. Ed.*, 2014, **53**, 11926.

15. T. Kajiwara, M. Fujii, M. Tsujimoto, K. Kobayashi, M. Higuchi, K. Tanaka and S. Kitagawa, *Angew. Chem. Int. Ed.,* 2016, **55**, 2697.

16. S. Sato, T. Morikawa, S. Saeki, T. Kajino and T. Motohiro, *Angew. Chem. Int. Ed.,* 2010, **49**, 5101.

17. R. Kuriki, H. Matsunaga, T. Nakashima, K. Wada, A. Yamakata, O. Ishitani and K. Maeda, *J. Am. Chem. Soc.,* 2016, **138**, 5159.

18. R. Kuriki, M. Yamamoto, K. Higuchi, Y. Yamamoto, M. Akatsuka, D. Lu, S. Yagi, T. Yoshida, O. Ishitani and K. Maeda, *Angew. Chem. Int. Ed.,* 2017, **56**, 4867.

19. H. Zhang, J. Wei, J. Dong, G. Liu, L. Shi, P. An, G. Zhao, J. Kong, X. Wang, X. Meng, J. Zhang and J. Ye, *Angew. Chem. Int. Ed.,* 2016, **55**, 14310.

20. L. Shi, T. Wang, H. Zhang, K. Chang and J. Ye, *Adv. Funct. Mater.,* 2015, **25**, 5360.

21. Y. Fu, D. Sun, Y. Chen, R. Huang, Z. Ding, X. Fu and Z. Li, *Angew. Chem. Int. Ed.,* 2012, **51**, 3364.

22. H. Q. Xu, J. Hu, D. Wang, Z. Li, Q. Zhang, Y. Luo, S. H. Yu and H. L. Jiang, *J. Am. Chem. Soc.,* 2015, **137**, 13440.